



Influence of Co and Ni addition on the magnetocaloric effect in Fe_{88-2x}Co_xNi_xZr₇B₄Cu₁ soft magnetic amorphous alloys

R. Caballero-Flores, V. Franco, A. Conde, K. E. Knipling, and M. A. Willard

Citation: [Applied Physics Letters](#) **96**, 182506 (2010); doi: 10.1063/1.3427439

View online: <http://dx.doi.org/10.1063/1.3427439>

View Table of Contents: <http://scitation.aip.org/content/aip/journal/apl/96/18?ver=pdfcov>

Published by the [AIP Publishing](#)

Articles you may be interested in

[Nanocrystalline Fe_{88-2x}Co_xNi_xZr₇B₄Cu₁ alloys: Soft magnets for vehicle electrification technologies \(invited\)](#)

[J. Appl. Phys.](#) **117**, 172611 (2015); 10.1063/1.4914118

[Magnetocaloric effect in Fe-Zr-B-M \(M=Ni, Co, Al, and Ti\) amorphous alloys](#)

[J. Appl. Phys.](#) **116**, 093910 (2014); 10.1063/1.4895048

[Magnetocaloric effect and critical exponents of Fe₇₇Co_{5.5}Ni_{5.5}Zr₇B₄Cu₁: A detailed study](#)

[J. Appl. Phys.](#) **109**, 07A905 (2011); 10.1063/1.3535191

[The magnetocaloric effect in soft magnetic amorphous alloys](#)

[J. Appl. Phys.](#) **101**, 09C503 (2007); 10.1063/1.2709409

[The influence of Co addition on the magnetocaloric effect of Nanoperm-type amorphous alloys](#)

[J. Appl. Phys.](#) **100**, 064307 (2006); 10.1063/1.2337871



NEW Special Topic Sections

NOW ONLINE
Lithium Niobate Properties and Applications:
Reviews of Emerging Trends

AIP Applied Physics Reviews

The advertisement features a blue background with a glowing light effect on the right. On the left, there is a small image of the journal cover for Applied Physics Reviews, which shows a 3D lattice structure and a graph. The text 'NEW Special Topic Sections' is prominently displayed in white. Below it, the text 'NOW ONLINE' is in yellow, followed by the title of the special topic section in white. The AIP logo and 'Applied Physics Reviews' are in the bottom right corner.

Influence of Co and Ni addition on the magnetocaloric effect in $\text{Fe}_{88-2x}\text{Co}_x\text{Ni}_x\text{Zr}_7\text{B}_4\text{Cu}_1$ soft magnetic amorphous alloys

R. Caballero-Flores,¹ V. Franco,^{1,a)} A. Conde,¹ K. E. Knipling,² and M. A. Willard²

¹Dpto. Física de la Materia Condensada, ICMSE-CSIC, Universidad de Sevilla, P.O. Box 1065, 41080 Sevilla, Spain

²Multifunctional Materials Branch, U.S. Naval Research Laboratory, 4555 Overlook Avenue, SW, Washington, DC 20375, USA

(Received 26 March 2010; accepted 19 April 2010; published online 7 May 2010)

We have studied the magnetocaloric effect in a series of $\text{Fe}_{88-2x}\text{Co}_x\text{Ni}_x\text{Zr}_7\text{B}_4\text{Cu}_1$ alloys. The partial substitution of Fe by Co and Ni leads to a monotonic increase in the Curie temperature (T_C) of the alloys from 287 K for $x=0$ to 626 K for $x=11$. The maximum magnetic entropy change (ΔS_M^{pk}) at an applied field of 1.5 T, shows a value of $1.98 \text{ J K}^{-1} \text{ kg}^{-1}$ for $x=8.25$. The refrigerant capacity (RC) has maximum values near 166 J kg^{-1} (for $x=0$ and 2.75). These values place the present series of alloys among the best magnetic refrigerant materials, with an RC $\sim 40\%$ larger than $\text{Gd}_5\text{Si}_2\text{Ge}_{1.9}\text{Fe}_{0.1}$ and $\sim 15\%$ larger than Fe-based amorphous alloys. © 2010 American Institute of Physics. [doi:10.1063/1.3427439]

Ambient-temperature solid-state magnetic refrigeration employing the magnetocaloric effect (MCE) is a field of active research.¹⁻³ Compared with conventional gas compression-expansion refrigeration, magnetic refrigeration based on MCE offers improved energy efficiency and reduced environmental impact.⁴ In magnetic materials, the MCE arises from the reversible temperature change that occurs during the application or removal of an external magnetic field H under adiabatic conditions. This temperature change is accompanied by a change in magnetic entropy (ΔS_M), leading to a refrigerant capacity (RC), which is defined as the heat transferred between the hot and cold reservoirs used in the ideal thermodynamic cycle. The RC depends both on the magnitude of ΔS_M (i.e., its peak value, ΔS_M^{pk}) as well as its temperature dependence (i.e., the width of the peak). An optimal refrigerant material maximizes both ΔS_M^{pk} and RC.

The largest ΔS_M^{pk} values generally occur in materials with a first order magnetostructural phase transition [e.g., $\text{Gd}_5(\text{Si}, \text{Ge})_4$, $\text{La}(\text{Fe}, \text{Si})_{13}$, FeMnPAs , etc].^{5,6} There are, however, several complications arising from the nature of the phase transition.^{7,8} These include the following: (i) the effects of thermal- and field-hysteresis,⁹ (ii) a large volume change and the concomitant stresses between the coexisting phases,^{10,11} (iii) magnetic degrees of freedom coupling with vibrational ones¹² producing additional contributions to MCE, and (iv) the slow kinetics of the first order transitions which can limit the performance of a refrigerator employing these materials.

Amorphous magnetic materials offer significant potential as magnetic refrigerant materials¹³⁻¹⁵ because they (i) undergo a second order magnetic phase transition which exhibits a broad ΔS_M peak around the Curie temperature T_C (Ref. 13) (in contrast with the usually narrow ΔS_M peak present in materials with first order phase transitions), (ii) provide tunable magnetic transition temperatures by alloying,¹⁶ (iii) present neither volume nor structural changes, and (iv) produce large RC,¹⁷ significantly reduced magnetic and thermal

hysteresis, high electrical resistivity, good mechanical properties, and an improved corrosion resistance. Rare earth based amorphous alloys have large values of ΔS_M^{pk} and RC, but their T_C is well below room temperature, making them unsuitable for ambient-temperature applications.¹⁸⁻²⁰ Iron-based (e.g., nanoperm-type Fe-Zr-B-Cu) alloys have a T_C close to room temperature (which can be further modified by alloying)²¹ and are much more affordable than rare earth based alloys, but their magnetocaloric response is comparatively much smaller.¹⁷ In this work it will be shown that the combined addition of Co and Ni to Fe-Zr-B-Cu type alloys leads to amorphous materials with large magnetocaloric response, surpassing the RC of the well known crystalline magnetic refrigerant $\text{Gd}_5\text{Si}_2\text{Ge}_{1.9}\text{Fe}_{0.1}$ by $\sim 40\%$ and a leading amorphous alloy, $\text{Fe}_{83}\text{Zr}_6\text{B}_{10}\text{Cu}_1$, by $\sim 15\%$.

Amorphous ribbons of $\text{Fe}_{88-2x}\text{Co}_x\text{Ni}_x\text{Zr}_7\text{B}_4\text{Cu}_1$ (typically 2–3 mm wide and $\sim 20 \mu\text{m}$ thick) with compositions corresponding to $x=0, 2.75, 5.5, 8.25$, and 11, were obtained by a melt-spinning technique. Further details about sample preparation, microstructural, and magnetic characterization are given elsewhere.²²

The change in magnetic entropy caused by a variation in applied magnetic field has been obtained by numerical approximation of

$$\Delta S_M(T, \Delta H) = \mu_0 \int_{H_0}^{H_f} \left[\frac{\partial M(T, H)}{\partial T} \right]_H dH, \quad (1)$$

where $\Delta H = H_f - H_0$ is the magnetic field change, μ_0 is the magnetic permeability of vacuum, and $M(T, H)$ is the magnetization of the material. The field and temperature dependence of $M(T, H)$ was measured (up to $\mu_0 H_{\text{max}} = 1.5 \text{ T}$ in 10 mT increments and from 100 to 713 K in 10 K increments) by vibrating sample magnetometry. Figure 1 shows the corresponding temperature dependence of ΔS_M at a maximum applied field of 1.5 T for the alloys studied. The curves have a caret-like shape, characteristic of a second order phase transition, which becomes sharper with increasing Co/Ni content.

RC can be calculated from ΔS_M according to

^{a)}Electronic mail: vfranco@us.es.

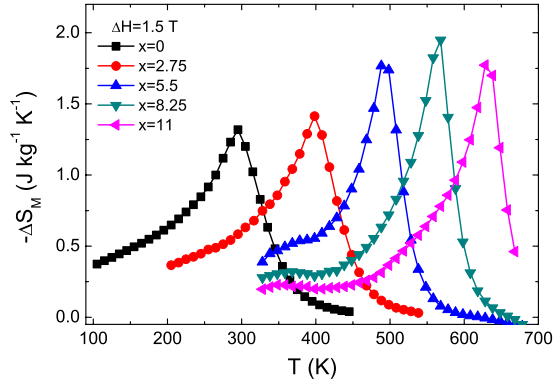


FIG. 1. (Color online) Temperature dependence of the magnetic entropy change corresponding to a magnetic field change $\Delta H=1.5$ T in the amorphous $\text{Fe}_{88-2x}\text{Co}_x\text{Ni}_4\text{Zr}_7\text{B}_4\text{Cu}_1$ ($x=0, 2.75, 5.5, 8.25, \text{ and } 11$) alloy series.

$$\text{RC}(\Delta H) = \int_{T_{\text{cold}}}^{T_{\text{hot}}} \Delta S_M(T, \Delta H) dT. \quad (2)$$

From the experimental data, this integral may be evaluated by a number of methods. RC_{AREA} is calculated by integrating ΔS_M across the temperature range spanning the half-maximum of the entropy change. RC_{FWHM} approximates the integral as the product of ΔS_M^{pk} with the same full width at half maximum (FWHM) temperature range. According to Wood and Potter,²³ RC_{WP} is taken as the area of the largest rectangle which can be inscribed inside the $\Delta S_M(T)$ curve. In this work all three definitions are used, to facilitate comparison with prior studies.

The compositional dependence of RC , ΔS_M^{pk} , and T_C is shown in Fig. 2 for the alloys studied. The values of T_C have been obtained from the inflection point of the experimental magnetization data at low field ($\mu_0 H_{\text{max}}=10$ mT). There is a monotonic increase in T_C from 287 K for $x=0$ to 626 K for $x=11$, which follows a power law defined as $T_C(x) \propto x^{0.81}$ ($r^2=0.999$). This empirically obtained power law can be used to fine tune the composition of the alloy for a desired T_C . The temperature at which ΔS_M^{pk} occurs (Fig. 1) correlates well to the value of T_C for each alloy. The compositional evolution of ΔS_M^{pk} , however does not show a power law behavior. For the extreme compositions of the series, ΔS_M^{pk} passes from $1.32 \text{ J K}^{-1} \text{ kg}^{-1}$ for $x=0$ to $1.81 \text{ J K}^{-1} \text{ kg}^{-1}$ for $x=11$, and is maximized for $x=8.25$ with a value of $1.98 \text{ J K}^{-1} \text{ kg}^{-1}$.

The RC_{FWHM} and RC_{AREA} have a stepwise behavior due to the much narrower peak widths of the alloys with $x \geq 5.5$. RC_{FWHM} varies abruptly from $\sim 166 \text{ J kg}^{-1}$ ($x=0$ and 2.75) to 130 J kg^{-1} ($x=5.5, 8.25, \text{ and } 11$). This is due to the different shapes of the low temperature tails of the $\Delta S_M(T)$ curves presented in Fig. 1. RC_{WP} , however, decreases monotonically from $\sim 95 \text{ J kg}^{-1}$ for $x=0$ to $\sim 73 \text{ J kg}^{-1}$ for $x=11$.

In order to compare these experimental values with those reported in the literature for other alloys, it would be necessary in most cases to formulate an expression to convert the values to an applied field of 5 T. It has been shown theoretically and experimentally that the field dependence of ΔS_M can be represented as^{24,25} $\Delta S_M(T, H) = c(T)H^n$. At $T=T_C$ and $T=T_{\text{pk}}$, the exponent n is field independent. At any other temperature, n is a function of the applied magnetic field.²⁶

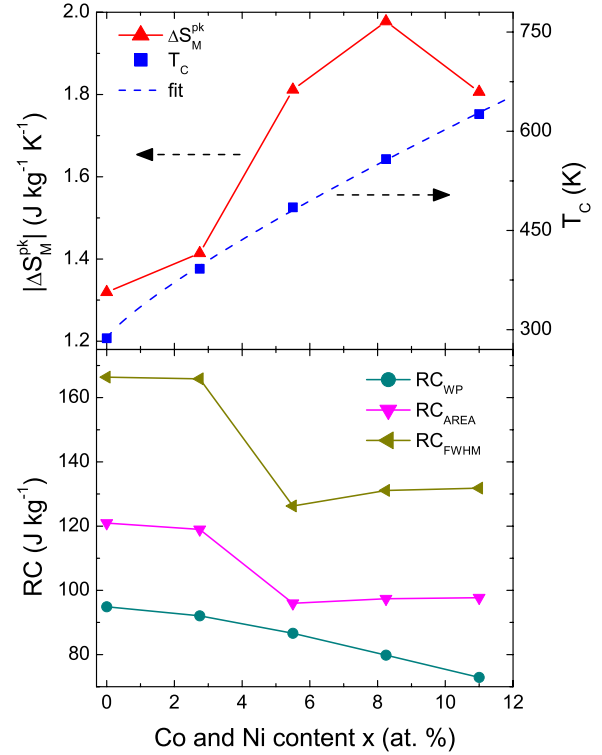


FIG. 2. (Color online) Dependence of the T_C , ΔS_M^{pk} , and the different RCs, RC_{WP} , RC_{AREA} , and RC_{FWHM} on the Co and Ni content of the amorphous $\text{Fe}_{88-2x}\text{Co}_x\text{Ni}_4\text{Zr}_7\text{B}_4\text{Cu}_1$ ($x=0, 2.75, 5.5, 8.25, \text{ and } 11$) alloy series. A magnetic field of $\mu_0 H_{\text{max}}=1.5$ T was employed to measure the ΔS_M^{pk} and RC values. Dashed line indicates the fitted data of T_C according to a power law $T_C(x) \propto x^{0.81}$ ($r^2=0.999$).

RC can also be expressed as a power law of the field: $\text{RC}(H) = bH^{n'}$.

By normalizing these expressions with the values corresponding to the maximum applied field, dimensionless relationships can be written for the different studied compositions

$$\delta s = \frac{\Delta S_M^{\text{pk}}(H, x)}{\Delta S_M^{\text{pk}}(H_{\text{max}}, x)} = \frac{a(x)H^n}{a(x)H_{\text{max}}^n} = h^n,$$

$$\text{rc} = \frac{\text{RC}_{\text{FWHM}}(H, x)}{\text{RC}_{\text{FWHM}}(H_{\text{max}}, x)} = \frac{b(x)H^{n'}}{b(x)H_{\text{max}}^{n'}} = h^{n'}, \quad (3)$$

where $h = H/H_{\text{max}}$. In principle, the exponents n and n' could be composition dependent (i.e., dependent on x). However, when these power laws are plotted for the different alloys (Fig. 3) both power law exponents have very similar values for the full series of alloys.

The present alloys compare favorably with other magnetocaloric materials. Among crystalline compounds, $\text{Gd}_5\text{Si}_2\text{Ge}_{1.9}\text{Fe}_{0.1}$ is one of the most prominent materials due to its reduced hysteresis. For an applied field of 5 T its RC_{AREA} is 355 J kg^{-1} ; when the values of the studied alloys are calculated at 5 T based on the power law relationship in Fig. 3, the two alloys with the transition temperatures closest to room temperature ($x=0$ and 2.75) have $\text{RC}_{\text{AREA}} = 496 \text{ J kg}^{-1}$, which is a $\sim 40\%$ increase. The values of ΔS_M^{pk} for the present alloys, which extrapolate to $5.3 \text{ J kg}^{-1} \text{ K}^{-1}$ for an applied field of 5 T, is smaller than that of $\text{Gd}_5\text{Si}_2\text{Ge}_{1.9}\text{Fe}_{0.1}$ ($7 \text{ J kg}^{-1} \text{ K}^{-1}$). The comparison with the

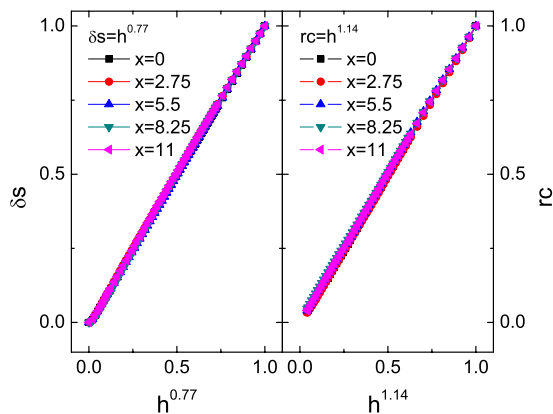


FIG. 3. (Color online) Dimensionless field dependence of the dimensionless peak entropy change, δs , and rc of the amorphous $\text{Fe}_{88-2x}\text{Co}_x\text{Ni}_x\text{Zr}_7\text{B}_4\text{Cu}_1$ ($x=0, 2.75, 5.5, 8.25,$ and 11) alloy series. The collapse into a single master curve indicates that exponents n and n' are composition independent. For $x=8.25$, rc has been calculated from the width at 60% of the peak (instead of width at half maximum) to avoid mixing experimental data from the cryostat and the furnace.

$\text{Fe}_{83}\text{Zr}_6\text{B}_{10}\text{Cu}_1$ amorphous alloy (the Fe-based amorphous alloy with largest RC reported to date) is also favorable.¹⁷ In that case, for an applied field of 1.5 T, $\text{RC}_{\text{AREA}} = 104 \text{ J kg}^{-1}$, indicating that the series of alloys studied in this work give an increase of $\sim 15\%$. In addition to this enhancement, with the present alloy series we have been able to tune the Curie temperature down to room temperature, while $\text{Fe}_{83}\text{Zr}_6\text{B}_{10}\text{Cu}_1$ had a $T_C = 398 \text{ K}$. The values of the peak entropy change for $\text{Fe}_{83}\text{Zr}_6\text{B}_{10}\text{Cu}_1$ and for the present series are similar.

In summary, it has been shown that by the simultaneous addition of Co and Ni to Fe–Zr–B–Cu alloys, the Curie temperature of the alloys can be tuned in a range which includes room temperature. The RC of this family of alloys is enhanced in $\sim 40\%$ with respect to the crystalline $\text{Gd}_5\text{Si}_2\text{Ge}_{1.9}\text{Fe}_{0.1}$ and $\sim 15\%$ with respect to the best Fe-based amorphous alloy reported so far. This makes these alloys promising candidates to be used as room temperature magnetic refrigerants.

This work was supported by the Spanish Ministry of Science and Innovation and EU FEDER (Project No. MAT 2007-65227), the PAI of the Regional Government of An-

dalucia (Project No. P06-FQM-01823), and by the United States Office of Naval Research (Contract No. N0001410WX30037). R. C. F. acknowledges a research fellowship from the Regional Government of Andalusia.

- ¹K. A. Gschneidner, Jr., V. K. Pecharsky, and A. O. Tsokol, *Rep. Prog. Phys.* **68**, 1479 (2005).
- ²E. Brück, *J. Phys. D: Appl. Phys.* **38**, R381 (2005).
- ³A. M. Tishin and Y. I. Spichkin, *The Magnetocaloric Effect and its Applications*, 1st ed. (Institute of Physics Publishing, Bristol, Philadelphia, 2003), p. 475.
- ⁴B. F. Yu, Q. Gao, B. Zhang, X. Z. Meng, and Z. Chen, *Int. J. Refrig.* **26**, 622 (2003).
- ⁵V. K. Pecharsky and K. A. Gschneidner, Jr., *Phys. Rev. Lett.* **78**, 4494 (1997).
- ⁶K. A. Gschneidner, Jr. and V. K. Pecharsky, *Annu. Rev. Mater. Sci.* **30**, 387 (2000).
- ⁷K. A. Gschneidner, Jr. and V. K. Pecharsky, *Int. J. Refrig.* **31**, 945 (2008).
- ⁸B. G. Shen, J. R. Sun, F. X. Hu, H. W. Zhang, and Z. H. Cheng, *Adv. Mater.* **21**, 4545 (2009).
- ⁹V. Provenzano, A. J. Shapiro, and R. D. Shull, *Nature (London)* **429**, 853 (2004).
- ¹⁰L. Morellon, P. A. Algarabel, M. R. Ibarra, J. Blasco, B. García-Landa, Z. Arnold, and F. Albertini, *Phys. Rev. B* **58**, R14721 (1998).
- ¹¹M. Nazih, A. De Visser, L. Zhang, O. Tegus, and E. Brück, *Solid State Commun.* **126**, 255 (2003).
- ¹²J. D. Zou, H. Wada, B. G. Shen, J. R. Sun, and W. Li, *Europhys. Lett.* **81**, 47002 (2008).
- ¹³L. Si, J. Ding, Y. Li, B. Yao, and H. Tan, *Appl. Phys. A: Mater. Sci. Process.* **75**, 535 (2002).
- ¹⁴V. Franco, J. S. Blázquez, C. F. Conde, and A. Conde, *Appl. Phys. Lett.* **88**, 042505 (2006).
- ¹⁵I. Skorvanek, J. Kovac, J. Marcin, P. Svec, and D. Janickovic, *Mater. Sci. Eng., A* **449–451**, 460 (2007).
- ¹⁶Y. Wang and X. Bi, *Appl. Phys. Lett.* **95**, 262501 (2009).
- ¹⁷V. Franco, J. S. Blázquez, and A. Conde, *J. Appl. Phys.* **100**, 064307 (2006).
- ¹⁸J. Du, Q. Zheng, Y. B. Li, Q. Zhang, D. Li, and Z. D. Zhang, *J. Appl. Phys.* **103**, 023918 (2008).
- ¹⁹Q. Y. Dong, B. G. Shen, J. Chen, J. Shen, F. Wang, H. W. Zhang, and J. R. Sun, *J. Appl. Phys.* **105**, 053908 (2009).
- ²⁰F. W. Wang, X. X. Zhang, and F. X. Hu, *Appl. Phys. Lett.* **77**, 1360 (2000).
- ²¹K. Suzuki and J. M. Cadogan, *J. Magn. Magn. Mater.* **203**, 229 (1999).
- ²²K. E. Knipling, M. Daniil, and M. A. Willard, *Appl. Phys. Lett.* **95**, 222516 (2009).
- ²³M. E. Wood, and W. H. Potter, *Cryogenics* **25**, 667 (1985).
- ²⁴V. Franco, A. Conde, J. M. Romero-Enrique, and J. S. Blázquez, *J. Phys.: Condens. Matter* **20**, 285207 (2008).
- ²⁵V. Franco and A. Conde, *Int. J. Refrig.* **33**, 465 (2010).
- ²⁶V. Franco, A. Conde, M. D. Kuz'Min and J. M. Romero-Enrique, *J. Appl. Phys.* **105**, 07A917 (2009).